Enhanced Junction Capacitance Modelling

Frederick G Anderson,* Robert M Rassel, and Mark A Lavoie

IBM Microelectronics, 1000 River St., Essex Junction, VT 05452
* fredand@us.ibm.com

ABSTRACT

Wireless technologies have led to an increased focus on varactor devices. The current standard diode junction capacitance models are barely suitable for use with hyperabrupt junction varactors. We propose here a simple VerilogA solution that is very physical in that it employs the dopant distribution coming from SIMS characterisation of the junction. This new methodology is shown to enhance the voltage range over which the model is accurate, is more physical which leads to better process statistics, and also accounts for temperature effects.

Keywords: junction varactor, capacitance, verilogA

1 INTRODUCTION

The proliferation of wireless technologies has placed an emphasis on VCO design that has in turn led to greater scrutiny of varactor models. One popular type of varactor is the hyperabrupt (HA) junction varactor. By tailoring various implants into the pn junction, a capacitance versus voltage (CV) curve that has an optimal shape for circuit design can be obtained. The problem for passive device modelers is to model this CV curve over a wide voltage range. The current models for junction capacitance are found in the standard diode models within various simulators. These models are based on a very simple power-law doping profile. The capacitance can be easily derived and written in a closed form expression. It is possible to employ such standard models to describe the CV relation found in the HA varactor, but the fitting region is barely sufficient and the extracted parameters can be non-physical. Hence, the modelling of this device is not physics-based, but is more an exercise in curve fitting using a very limiting expression. The additional features that make a model of higher quality, such as the dependence of the capacitance on temperature or on processing parameters, are even more difficult to model since the model parameters are not really tied to anything physical but are simply curve fitting parameters.

We offer here a relatively simple fix to this situation. We employ the doping density that results from a SIMS characterisation of the junction in order to get a much more accurate doping distribution. In the case of the HA varactor, this distribution is the result of several doping distributions. The Principle of Superposition in electrostatics allows us to treat each of these distributions independently and simply sum their individual effects. It is then a simple matter within VerilogA to arrive at a self-consistent solution using this sum of individual contributions.

In the next section, we detail the expressions that are used in our calculations. The derivation of these expression follow the well known procedures associated with the electrostatiscs of pn junctions. We then show how our methodology improves the modelling of a typical CV curve for a HA varactor. We also show how temperature shifts are taken into account. Lastly, we discuss more of the advantages and disadvantages of this methodology.

2 THEORY

We examine here an improvement to using the standard diode model. The standard junction diode capacitance, and we will only focus on the area term in this work, is given by (See for example [1])

$$C(V) = \frac{C_o}{\left(1 - \frac{V}{V_{bi}}\right)^m} \tag{1}$$

where C_o is the capacitance with zero volts across the junction, V_{bi} is the built-in potential across the junction, and m is determined from the power-law function that describes the doping distribution. If the dopant density (n) is given by the expression $n = x^p$, where x is the distance from the actual pn junction, then $m = 1/(p+2)$. We note that this expression makes the assumption that one side of the junction is so heavily doped that it does not contribute to the size of the depletion region. Our new methodology does not make this assumption, and so is more general.

The expression in (1) gives the general qualitative shape of the CV curve found for an HA varactor. However, the voltage range of the fit is barely sufficient. This is a result of the dopant distribution inside the HA varactor. A typical HA varactor is shown in Fig. 1. It consists of a heavily doped p-region for the anode and

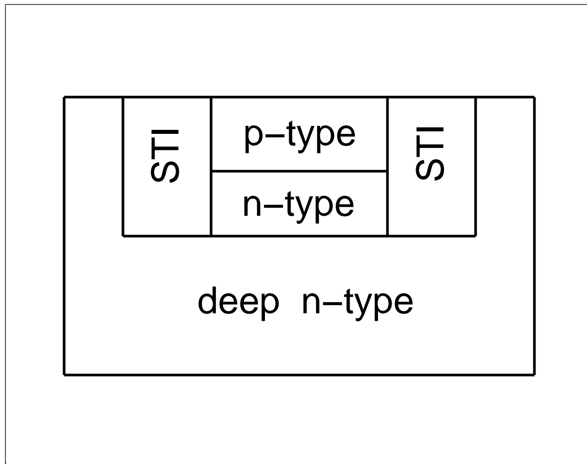

Figure 1: Schematic layout of HA varactor showing heavily doped p-type region at surface, an n-type implant forming the hyperabrupt junction, and a deeper n-type region.

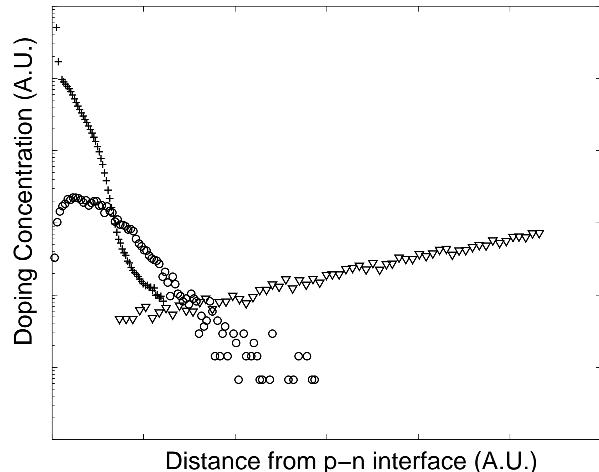

Figure 2: SIMS profile for HA varactor. The surface has p-type implant (+). At the junction is an n-type implant to make this hyperabrupt (o). Lastly, a deep n-type implant (triangles) enhances the quality factor.

a less strongly doped n-region for the cathode. The n-type implants are divided into two parts: (1) an implant at the junction itself to make the device "hyperabrupt," and (2) a deeper implant to lower the resistance of the cathode in order to enhance the quality factor of the device. So, already, we know that the doping density is not going to follow a simple power-law function. The SIMS profile of the junction yields insight into the doping density. As shown in Fig. 2, the doping density clearly does not follow a power-law distribution but is very nearly piecewise exponential.

As the doping density is clearly not a power-law function of depth, we conclude that the use of the standard junction capacitance model is at best an exercise in curve fitting. The result of this exercise is that the parameters in (1) have lost their physical meaning, and indeed non-physical values often result from this fit. Experience shows however that the simple expression in (1) can be used over a portion of the CV curve, but that this region is fairly limited. Our new methodology is the result of a request from designers to increase the voltage range of the validity of the model.

The new methodology we are proposing in this work is possible through VerilogA, which is now available in the primary simulation tools. The use of VerilogA for varactor modelling requires finding Q, the "stored charge" on the plates.[2] One then determines the current using the *ddt* time differential operator. To get the total charge, one simply integrates the distribution over the depletion region. Hence, we need to know the size of the depletion region. This can be determined by setting the voltage across the depletion region equal to the sum of the built-in potential and the applied potential. We adjust the size of the depletion region until this requirement of self-consistency is satisfied.

We can see from Fig. 2, that the total dopant density is made up of several distributions that are each exponential over the region of interest. Using the Principle of Superposition, each distribution can be treated separately. The total voltage across the depletion region V_d is the sum of voltages arising from each individual distribution $V_i, i = 1, 2, ...$

The ith doping distribution $n_i(x)$ is given by

$$n_i(x) = \alpha_i e^{\kappa_i x}. \tag{2}$$

Using Gauss's Law, we find the electric displacement field due to the ith distribution

$$D_i(x) = \pm q \alpha_i \left(e^{\kappa_i x} - e^{\kappa_i x_D} \right), \tag{3}$$

where $\pm q$ is the unit charge with the appropriate sign (+ for donors), and x_D is the size of the depletion region, where we define the pn junction to be at $x = 0$ with the positve x-direction being in the cathode region. A second integration yields the potential difference due to this i^{th} dopant between the end of the depletion region and $x = 0$

$$\begin{aligned} V_i &\equiv V_i(x_D) - V_i(0) \\ &= \frac{\pm q \alpha_i}{\kappa_i^2 \epsilon_o \epsilon_r} \left[1 - (1 - \kappa_i x_D) e^{\kappa_i x_D} \right]. \end{aligned} \tag{4}$$

We note that there are two values of x_D, one for the anode side of the junction and one for the cathode side. There is, of course, the usual constraint equation that the D field across $x = 0$ must be continuous. Hence, the sum of the D_i coming from the anode region must equal the sum of the D_i coming from the cathode region. Typically, there is a single dopant type in the anode

region, in contrast to the cathode region in which there are several implants. This situation results in a closed-form expression for x_{Dp} in terms of x_{Dn}

$$x_{Dp} = \frac{1}{\kappa_{anode}} \ln \left[1 + \frac{\kappa_{anode}}{q\alpha_{anode}} \sum_{i=cathode} D_i \right]. \qquad (5)$$

If this is not the case, then we must resort to numerical methods to determine x_{Dp} from x_{Dn}.

Since we can express x_{Dp} in terms of x_{Dn}, the problem is then one of determining the value of x_{Dn} that yields the proper voltage across the entire depletion region, one that equals the sum of the built-in potential and the applied potential. This problem is readily solved using the Newton-Raphson method. The derivatives of the potential functions are easy to determine. One must take some care however with the derivative of potential across the anode portion of the depletion region,

$$\frac{dV_{anode}}{dx_{Dn}} = \frac{dV_p}{dx_{Dp}} \frac{dx_{Dp}}{dx_{Dn}}. \qquad (6)$$

There are of course other methods to determine the value of x_{Dn} so that the potential across the depletion region equals the sum of the built-in potential and the applied potential, e.g., bisection algorithms that ar known to converge very rapidly. However, we have found that such methods give rise to "Hidden State Errors" within VerilogA when performing Periodic Steady State analyses.

Once the self-consistent value of x_{Dn} has been determined, the charge stored on the plates is simply given by the area of capacitor times the electric displacement field at the *pn* junction. We then apply the VerilogA *ddt* operator to this value of charge to determine the current through the capacitor.

3 RESULTS

The advantage of the method we have outlined here is that it is much more physical and yields a better fit to the data than the standard junction capacitance model. This is shown in Fig. 3. In this figure, we show the data as circles. The dotted line is the result of the best fit using the standard junction capacitance model. We see how it starts to deviate appreciably from the data for bias values greater than 3 volts reverse bias. As such, this methodology is barely sufficient for use by circuit designers. The results from our method are shown as the solid line. As one can see, this line follows the data very well as far as 6 volts reverse bias, which is only a few volts from the junction breakdown voltage.

Further, this method gives accurate results with change in temperature. If we assume that the dopants are completely ionised at all temperatures in the range of interest, then the only parameter in our model that is adjustable is the built-in potential, V_{bi}. The curves

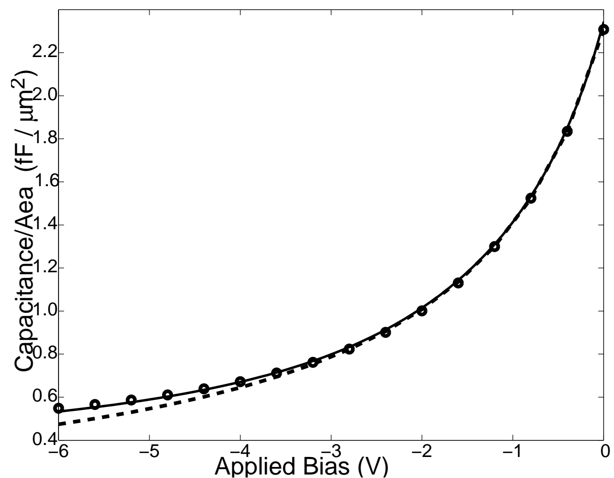

Figure 3: Capacitance per unit area of the HA varactor. The circles represent hardware characterisation. The dashed line is the result of the fit using the standard junction capacitance model; and the solid line is the fit resulting from the model we have detailed in this work.

in Fig. 4 show the results of only adjusting V_{bi} in a linear fashion with temperature. The upper curve gives the results at 125 C (our fit as the solid line and the data as circles). The middle curve gives the results at 25 C and the lower curve gives the results at -40 C. One can see how good the fit is over this temperature range. Of course, it is possible to tweak the doping concentrations α_i to account for changes with temperature in the number of ionised dopants.

4 CONCLUSION

We have proposed a new methodology to model the capacitance variation with reverse bias for the HA varactor. The importance of this device in wireless design has led to the increased need for a higher quality model, like the one we have detailed in this work. This model is completely physics based, as we have shown in the derivation, and uses as inputs the doping concentrations for the electrically important dopants. Hence, there is a direct link between the model parameters and the processing variations. This leads to accurate statistical models that track process variation as well as higher quality fits to the CV curves. There is of course some concern about how to hide proprietary process infomation within the model, since the doping information is part of the model inputs. This can be handled to some degree by redefining the unit length from meters to some very arbitrary unit and then rescaling all of the model inputs and physical constants, α_i, κ_i, and ϵ_o. The availability of VerilogA in all of the most common simulators has allowed this kind of modelling to be possible and opens a whole range of possibilites for new device modelling methodologies.

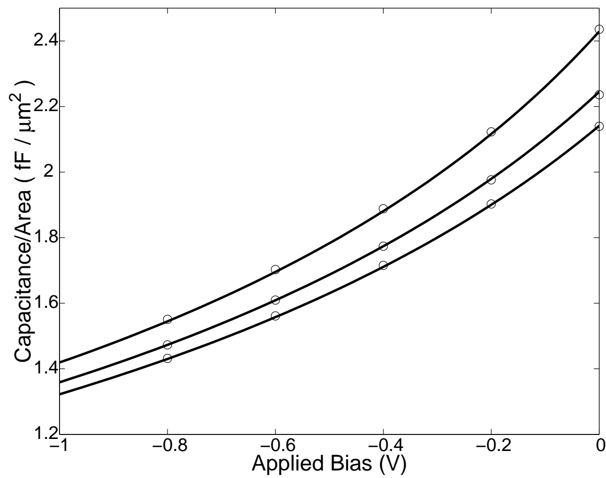

Figure 4: Plot showing the temperature dependence of the HA varactor CV curve at low reverse bias values, to show more detail. The circles represent hardware characterisation results and the solid lines the results from our proposed model in which only V_{bi} is varied in a linear fashion. Data was taken at 125, 25, and -40 C.

REFERENCES

[1] R. F. Pierret, "Semiconductor Device Fundamentals," Addison Wesley, 305-307, 1996.

[2] K. Kundert, "Modeling Varactors," Cadence Design Systems, June 2002. [Online]. Available: http://www.designers-guide.com/Modeling/varactors.pdf